nature genetics

Nras loss induces metastatic conversion of *Rb1*-deficient neuroendocrine thyroid tumor

Chiaki Takahashi[1,2,5,6], Bernardo Contreras[1,2], Tsuyoshi Iwanaga[5], Yujiro Takegami[6], Anke Bakker[7], Roderick T Bronson[4,8], Makoto Noda[6], Massimo Loda[1,3], Jennifer L Hunt[7] & Mark E Ewen[1,2]

Mutations in the gene encoding the retinoblastoma tumor suppressor predispose humans and mice to tumor development[1,2]. Here we have assessed the effect of *Nras* loss on tumor development in *Rb1* heterozygous mice. Loss of one or two *Nras* alleles is shown to significantly reduce the severity of pituitary tumors arising in *Rb1*$^{+/-}$ animals by enhancing their differentiation. By contrast, C-cell thyroid adenomas occurring in *Rb1*$^{+/-}$ mice progress to metastatic medullary carcinomas after loss of *Nras*. In *Rb1*$^{+/-}$*Nras*$^{+/-}$ animals, distant medullary thyroid carcinoma metastases are associated with loss of the remaining wild-type *Nras* allele. Loss of *Nras* in *Rb1*-deficient C cells results in elevated Ras homolog family A (RhoA) activity, and this is causally linked to the invasiveness and metastatic behavior of these cells. These findings suggest that the loss of the proto-oncogene *Nras* in certain cellular contexts can promote malignant tumor progression.

The involvement of the mutant forms of the Ras proto-oncogenes in tumorigenesis is well documented. In tumors harboring constitutively active Ras, the presence of wild-type Ras can affect tumor progression[3]. By contrast, little is known about the contribution of wild-type Ras to tumorigenesis in the absence of the mutant, oncogenic forms of Ras. To address this issue, we have asked whether loss of *Nras* affects tumor development in *Rb1* heterozygotes. Previous studies have shown that Ras is a downstream effector of pRb during differentiation[4], and that nullizygosity for *Nras* rescues a subset of developmental defects in *Rb1*-deficient embryos by affecting differentiation but not proliferation[5].

Rb1 heterozygotes develop pituitary adenocarcinomas and medullary thyroid (C-cell) adenomas. Both of these tumor types display a requirement for somatic loss of the remaining wild-type *Rb1* allele[6,7]. *Nras* nullizygous animals are normal and not tumor prone[8]. To

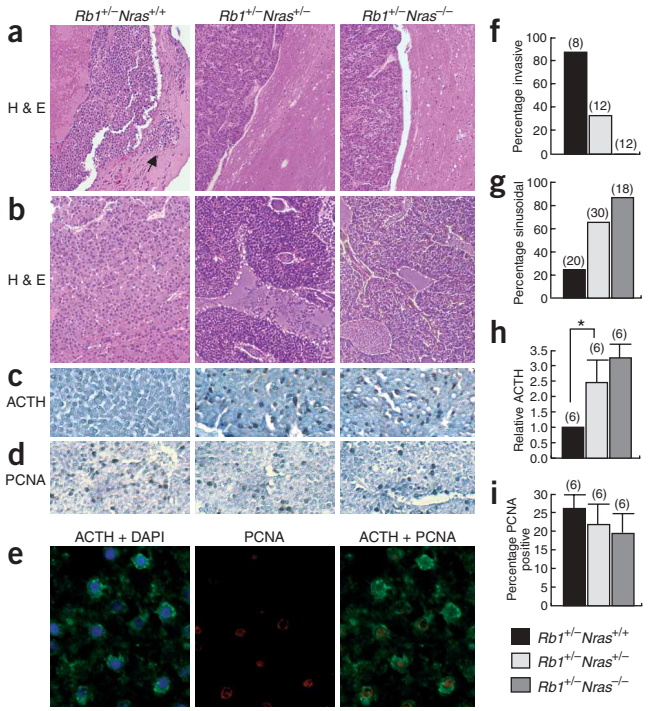

Figure 1 Effects of *Nras* loss on pituitary tumor formation in *Rb1*$^{+/-}$ mice. (**a**–**d**) Sections from pituitary tumors arising in mice of the indicated genotype stained with H&E (**a**,**b**) or immunostained with antibody to ACTH (**c**) or PCNA (**d**). Arrow in **a** is to the invasive front of the tumor. Magnification, 10× (**a**); 20× (**b**); 40× (**c**,**d**). (**e**) Immunofluorescence of pituitary tumors arising in *Rb1*$^{+/-}$*Nras*$^{-/-}$ mice stained for ACTH (green) and DAPI (blue) (left), PCNA (red) (middle). Colocalization of ACTH and PCNA is shown in the merged image (right). (**f**,**g**) Frequency of appearance of invasive (**f**) versus sinusoidal (**g**) patterns of growth for pituitary tumors occurring in mice of the indicated genotype. Number of mice analyzed is in parentheses. (**h**,**i**) Quantification of ACTH (**h**) and PCNA (**i**) immunostaining for pituitary tumors occurring in mice of the indicated genotype. Results are means ± s.d. $^*P = 0.004$. Number of mice analyzed is in parentheses.

[1]Department of Medical Oncology, Dana-Farber Cancer Institute, [2]Department of Medicine, [3]Department of Pathology, [4]Rodent Histopathology Core, Harvard Medical School, Boston, Massachusetts 02115, USA. [5]The 21st Century Center of Excellence Program, [6]Department of Molecular Oncology, Kyoto University Graduate School of Medicine, Kyoto, 606-8501, Japan. [7]Department of Pathology, University of Pittsburgh Medical Center, Pittsburgh, Pennsylvania 15213, USA. [8]Tufts University School of Veterinary Medicine, North Grafton, Massachusetts 01536, USA. Correspondence and requests for materials should be addressed to M.E.E. (mark_ewen@dfci.harvard.edu) or C.T. (chtakaha@virus.kyoto-u.ac.jp).

Received 12 September; accepted 13 October; published online 20 December 2005; doi:10.1038/ng1703

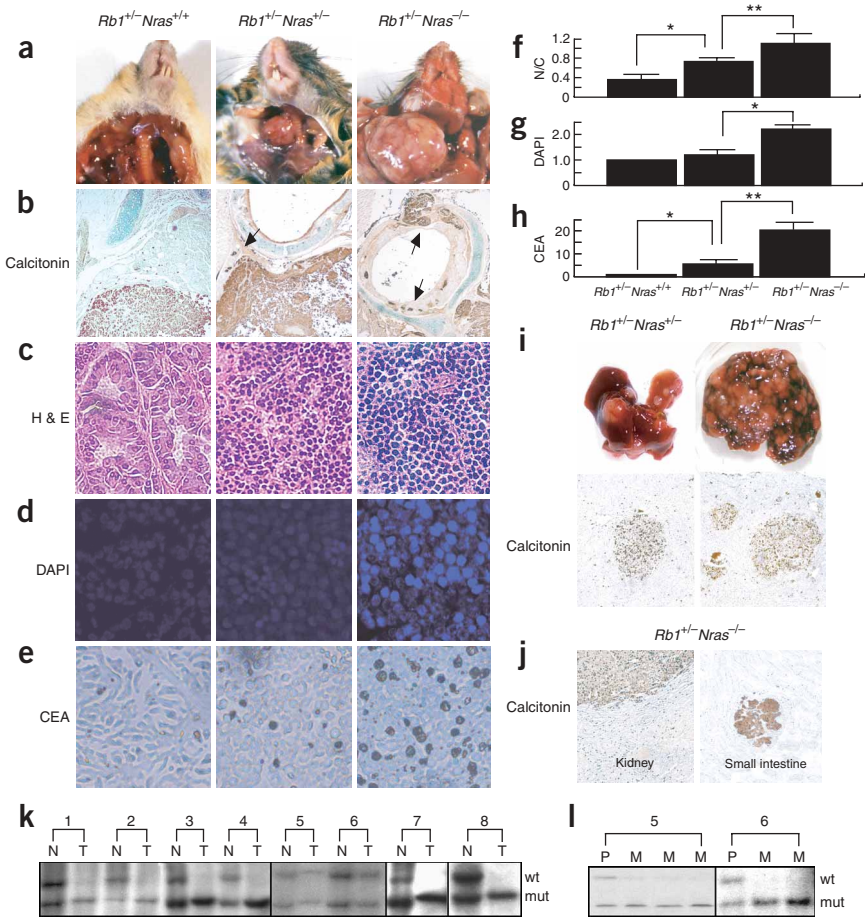

Figure 2 Contribution of *Nras* loss to C-cell thyroid tumor progression and metastasis in *Rb1*$^{+/-}$ mice. (**a**) Photographs of tracheal region of mice of the indicated genotype. Shown are macroscopic tumors arising in *Rb1*$^{+/-}$ *Nras*$^{+/-}$ and *Rb1*$^{+/-}$ *Nras*$^{-/-}$ animals, which do not occur in *Rb1*$^{+/-}$ mice. (**b**) Calcitonin-immunostained sections of C-cell tumors arising in mice of the indicated genotype. Arrows are drawn to tumor invasion into neighboring thyroid gland, perithyroidal soft tissue or trachea. Note that dispersed calcitonin-positive cells appearing in the thyroid gland of *Rb1*$^{+/-}$*Nras*$^{+/+}$ mice are normal C cells. Magnification, 10×. (**c**) H&E staining of sections of C-cell tumors arising in mice of the indicated genotype. Magnification, 40×. (**d**) 4′,6-diamidino-2-phenylindole (DAPI) staining of sections of C-cell tumors arising in mice of the indicated genotype. Magnification, 63×. (**e**) CEA-immunostained sections of C-cell tumors arising in mice of the indicated genotype. Magnification, 63×. (**f**) Quantification of the nuclear to cytoplasmic ratio (N/C) for H&E–stained sections of tumors arising in fifteen mice, five for each of the indicated genotypes. Results are means ± s.d. $*P = 0.002$; $**P = 0.003$. (**g**) Quantification of DAPI signal in C-cell tumors arising in fifteen mice, five for each of the indicated genotypes. Results are means ± s.d. $*P = 0.001$. (**h**) Quantification of CEA immunostaining for C-cell tumors arising in fifteen mice, five for each of the indicated genotypes. Results are means ± s.d. $*P < 0.001$; $**P < 0.001$. (**i**) Photograph (upper panels) and calcitonin-immunostained sections (lower panels) of liver metastases occurring in mice of the indicated genotype. Magnification, 10×. (**j**) Calcitonin-immunostained sections of C-cell tumor metastases to the kidney (left) and small intestine (right) occurring in *Rb1 Nras* mutant mice. Magnification, 10×. (**k**) Analysis of *Nras* locus by Southern blot analysis in primary C-cell tumors occurring in *Rb1*$^{+/-}$ *Nras*$^{+/-}$ mice; N, normal tail DNA; T, tumor DNA; wt, mut, wild-type and mutant *Nras* alleles, respectively. Tumors 1–4, 7 and 8 show loss of the remaining wild-type *Nras* allele. (**l**) Analysis of *Nras* locus by Southern blot analysis in C-cell tumor metastases occurring in *Rb1*$^{+/-}$ *Nras*$^{+/-}$ mice; P, primary tumor DNA; M, DNA derived from individual metastases; wt, mut, wild-type and mutant *Nras* alleles, respectively.

examine the genetic interaction between *Rb1* and *Nras* in tumor development, we crossed *Rb1*$^{+/-}$*Nras*$^{+/-}$ mice and analyzed and compared the resulting *Rb1*$^{+/-}$*Nras*$^{+/-}$, *Rb1*$^{+/-}$*Nras*$^{-/-}$ animals to *Rb1*$^{+/-}$*Nras*$^{+/+}$ littermates. All *Rb1*$^{+/-}$ mice (23/23) developed grossly detectable pituitary tumors, consistent with previous findings[6,9,10]. In contrast, only 47% of *Rb1*$^{+/-}$*Nras*$^{-/-}$ animals (16/38) showed evidence of pituitary tumors. *Rb1*$^{+/-}$ mice lacking a single *Nras* allele displayed an intermediate frequency (76%; 47/62) of grossly detectable pituitary tumors. The diameter of tumors arising in *Rb1*$^{+/-}$ mice was three to four times larger than those occurring in *Rb1*$^{+/-}$*Nras*$^{-/-}$ animals; tumors in *Rb1*$^{+/-}$*Nras*$^{+/-}$ mice were of intermediate size. The reduced penetrance and size of macroscopic pituitary tumors in *Rb1*$^{+/-}$*Nras*$^{-/-}$ and *Rb1*$^{+/-}$*Nras*$^{+/-}$ animals compared with those in *Rb1*$^{+/-}$ were not due to these mice being analyzed earlier, as their lifespan on average was longer than *Rb1*$^{+/-}$ mice (**Supplementary Fig. 1a**). Indeed, phenotypic analysis of these mice near the time of death suggests that a significant extension in lifespan resulting from loss of *Nras* was likely precluded due to the development of large thyroid tumors (**Supplementary Fig. 1b**; see below). Further, loss of the remaining wild-type *Rb1* allele was an invariant event in the development of pituitary tumors, regardless of *Nras* status (data not shown). These observations suggest that loss of one or both alleles of *Nras* delays the initiation or progression of pituitary tumors resulting from *Rb1* loss.

To understand why loss of *Nras* suppressed pituitary tumor formation in *Rb1* heterozygotes, we performed histological analyses. Hematoxylin and eosin (H&E) staining of pituitary tumors arising in *Rb1*$^{+/-}$ mice revealed a diffuse, poorly differentiated pattern of growth in which the normal lobular architecture was lost with obvious signs of local invasiveness (**Fig. 1a**,**b**,**f**,**g**). In contrast, tumors occurring in *Rb1*$^{+/-}$*Nras*$^{-/-}$ and *Rb1*$^{+/-}$*Nras*$^{+/-}$ animals displayed a differentiated sinusoidal pattern of growth with a well-confined architecture with pushing, noninfiltrating borders (**Fig. 1a**,**b**,**f**,**g**). Previous reports showed that adrenocorticotropic hormone (ACTH) is associated with differentiation[11], the expression levels of which inversely correlate with the aggressiveness of pituitary adenocarcinomas[12]. Consistent with the morphological characterization of pituitary tumors, ACTH levels were higher in tumors arising in *Rb1*$^{+/-}$*Nras*$^{-/-}$ and *Rb1*$^{+/-}$*Nras*$^{+/-}$ mice compared to those occurring in *Rb1*$^{+/-}$ animals (**Fig. 1c**,**h**). Staining for proliferating cell nuclear antigen (PCNA) to analyze the growth fraction did not reveal a significant difference in tumors arising in mice of all three genetic backgrounds (**Fig. 1d**,**i**). Proliferating cells (PCNA-positive) were also positive for ACTH

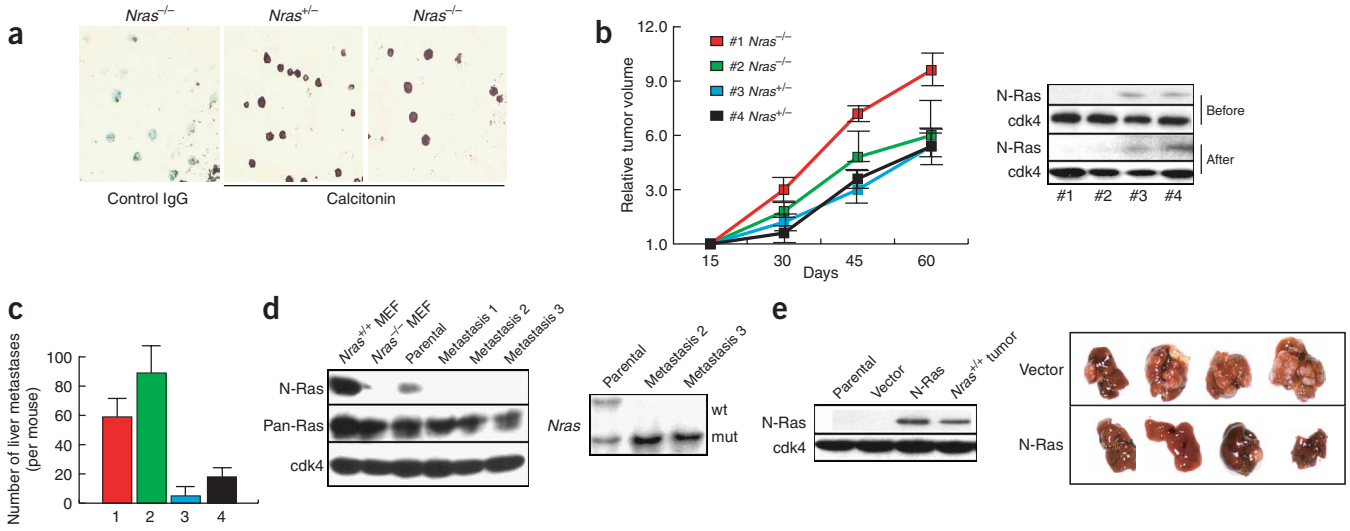

Figure 3 Contribution of *Nras* nullizygosity to the metastatic behavior of *Rb1*-deficient C cells. (**a**) Calcitonin immunostaining of C-cell cultures with the indicated genotypes and control IgG staining. (**b**) Growth kinetics of four C-cell lines of the indicated *Nras* genotype after subcutaneous injection of 5×10^6 cells. Tumor volume was determined using Vernier calipers. Each line was injected into five mice and the relative mean volume ± s.d. is shown (upper panel). N-Ras protein expression was assessed in C-cell lines before subcutaneous injection (Before) and from the resultant subcutaneous tumors (After) by immunoblotting (lower panel). Cdk4 immunoblots were used to assess protein loading. (**c**) Total number of liver metastatic nodules counted under a dissection microscope after intravenous injection of C cells (1×10^6) of the indicated *Nras* genotype (same lines as in panel **b**) into nude mice killed 2 months after injection. Each cell line was injected into ten mice and results are means ± s.d. (**d**) N-Ras protein expression (upper panel) and analysis of *Nras* locus by Southern blotting (lower panel) of $Rb1^{-/-}$ $Nras^{+/-}$ C cells before (Parental) and after (Metastasis) intravenous injection into nude mice. $Nras^{+/+}$ and $Nras^{-/-}$ MEFs were used as controls for N-Ras expression, whereas pan-Ras and cdk4 immunoblots were used as loading controls. Results are representative of three independent experiments. (**e**) N-Ras protein expression (immunoblot) after infection of $Rb1^{-/-}$ $Nras^{-/-}$ C cells with a lentivirus encoding N-Ras or empty vector (Vector), with cdk4 and a primary $Nras^{+/+}$ C-cell tumor used for loading controls (upper panel). Pictures of livers at 2 months after injection into the tail veins of nude mice with N-Ras reconstituted (N-Ras) or vector-infected (Vector) $Rb1^{-/-}$ $Nras^{-/-}$ C cells (1×10^6) (lower panel). Results shown are representative of 15 experiments, performed with two C-cell lines derived from different mice.

(**Fig. 1e**), suggesting that the genetic interaction between *Nras* and *Rb1* affects the differentiation status of pituitary tumor cells independently of their proliferative state. Together, these observations suggest that *Nras* nullizygosity reduces the penetrance of pituitary tumor development resulting from *Rb1* loss by maintaining a more differentiated phenotype, and further that *Nras* is haplo-insufficient for initiation or progression of pituitary tumors.

A substantial percentage of $Rb1^{+/-}Nras^{-/-}$ and $Rb1^{+/-}Nras^{+/-}$ mice developed palpable tumors in their tracheal region; this was not observed with *Rb1* heterozygotes (**Fig. 2a**). Thirty-three of the thirty-six $Rb1^{+/-}Nras^{-/-}$ mice analyzed had macroscopic tumors and of these the average weight was 198 mg. $Rb1^{+/-}Nras^{+/-}$ animals also developed large tumors albeit at a lower frequency (28/56) with an average weight of 164 mg. In contrast, 6 of 19 *Rb1* heterozygous mice had macroscopic tumors with the average weight being only 11 mg. Tumors arising in $Rb1^{+/-}Nras^{-/-}$ and $Rb1^{+/-}Nras^{+/-}$ mice were medullary carcinomas that were centered on the thyroid gland as revealed by histological examination. Their C-cell origin was confirmed by their neuroendocrine appearance and positive calcitonin staining (**Fig. 2b,c**). These tumors displayed an invasive pattern of growth where the entire lobe was filled, with extrathyroidal extension into the perithyroidal soft tissues being common. In contrast, tumors occurring in $Rb1^{+/-}$ animals were well circumscribed, indicative of their being adenomas. Nuclear to cytoplasmic ratio and nuclear features have been used to grade human thyroid C-cell tumors based upon their differentiation status, and together with the expression of carcinoembryonic antigen (CEA) to categorize them histologically as C-cell adenomas or carcinomas[13–15]. As in humans, tumors arising in $Rb1^{+/-}Nras^{-/-}$ and $Rb1^{+/-}Nras^{+/-}$ mice were carcinomas with poor differentiation, an increased nuclear to cytoplasmic ratio, hyperchromatic nuclei and CEA expression, as opposed to those occurring in $Rb1^{+/-}$ animals, which were adenomas (**Fig. 2c–h**). The observed tumor phenotypes are unlikely to be due to strain-specific differences as we have made similar observations after backcrossing five generations onto C57BL/6 or 129/Sv genetic backgrounds. However, we have not observed the development of malignant thyroid tumors in $Rb1^{+/-}$ mice that are heterozygous for *Kras*[16], suggesting that the effect of *Nras* on this tumor type may be Ras isoform–specific. These observations suggest that loss of one or two *Nras* alleles in $Rb1^{+/-}$ animals, in contrast to pituitary tumorigenesis, promotes the progression of thyroid C-cell tumors from adenomas to less differentiated aggressive carcinomas.

Full histological analysis of $Rb1^{+/-}Nras^{-/-}$ and $Rb1^{+/-}Nras^{+/-}$ mice did not reveal the presence of tumor types other than those that occur in *Rb1* heterozygotes. However, a significant fraction of $Rb1^{+/-}Nras^{-/-}$ (16/33) and $Rb1^{+/-}Nras^{+/-}$ (9/28) animals with macroscopic thyroid tumors showed evidence of distant medullary carcinoma metastases to the liver, lung, kidney, small intestine and adrenal glands, and less frequently to the brain and pleura (**Fig. 2i,j**; data not shown). In contrast, no metastatic lesions were noted in *Rb1* heterozygotes. These observations suggest that *Nras* nullizygosity or heterozygosity encourages the malignant conversion of C-cell adenomas in $Rb1^{+/-}$ mice.

The greater frequency of macroscopic C-cell tumors and associated metastases in $Rb1^{+/-}Nras^{-/-}$ compared to $Rb1^{+/-}Nras^{+/-}$ mice suggested that either *Nras* was haplo-insufficient for tumor suppression or in *Nras* heterozygotes the remaining wild-type *Nras* allele was lost. Southern blot analysis revealed that 8 of 22 tumors arising in

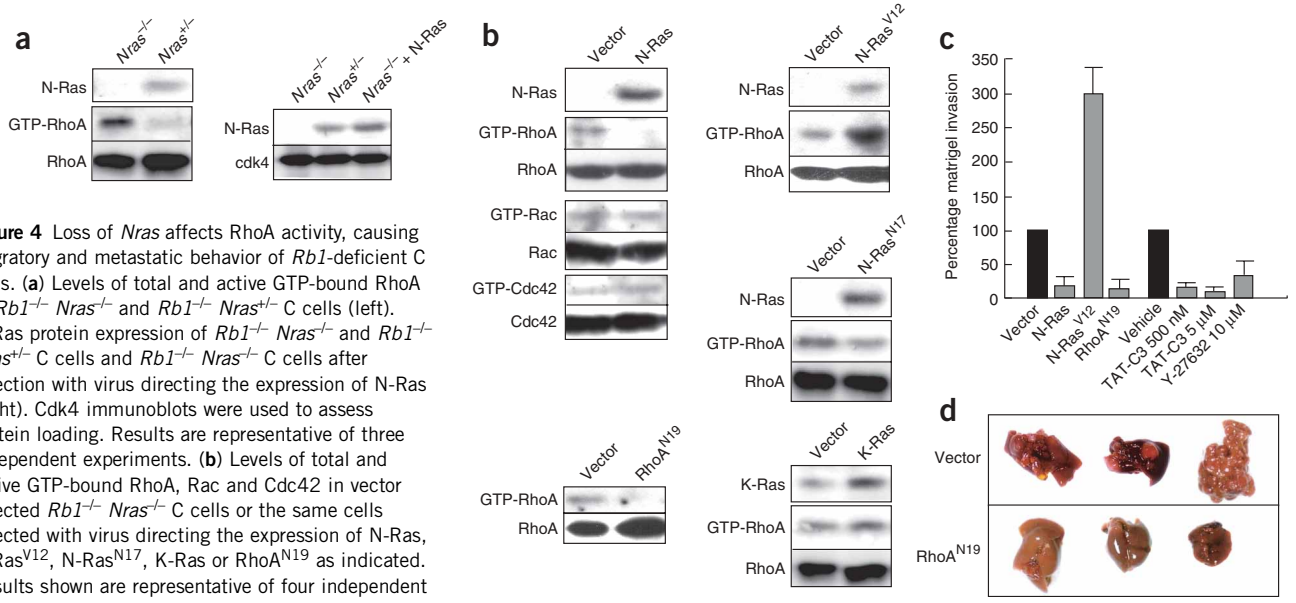

Figure 4 Loss of *Nras* affects RhoA activity, causing migratory and metastatic behavior of *Rb1*-deficient C cells. (**a**) Levels of total and active GTP-bound RhoA in $Rb1^{-/-}$ $Nras^{-/-}$ and $Rb1^{-/-}$ $Nras^{+/-}$ C cells (left). N-Ras protein expression of $Rb1^{-/-}$ $Nras^{-/-}$ and $Rb1^{-/-}$ $Nras^{+/-}$ C cells and $Rb1^{-/-}$ $Nras^{-/-}$ C cells after infection with virus directing the expression of N-Ras (right). Cdk4 immunoblots were used to assess protein loading. Results are representative of three independent experiments. (**b**) Levels of total and active GTP-bound RhoA, Rac and Cdc42 in vector infected $Rb1^{-/-}$ $Nras^{-/-}$ C cells or the same cells infected with virus directing the expression of N-Ras, N-Ras^{V12}, N-Ras^{N17}, K-Ras or $RhoA^{N19}$ as indicated. Results shown are representative of four independent experiments. (**c**) Invasion assays performed with $Rb1^{-/-}$ $Nras^{-/-}$ C cells (Vector or Vehicle controls) or the same cells either expressing N-Ras, N-Ras^{V12} or $RhoA^{N19}$, or treated with TAT-C3 or Y-27632 at the indicated concentrations before plating them. Results, mean ± s.d. for six independent experiments, are presented as percent of control cells that invade. (**d**) Pictures of livers at 2 months after intravenous injection into nude mice with $Rb1^{-/-}$ $Nras^{-/-}$ C cells (1×10^6) expressing $RhoA^{N19}$ ($RhoA^{N19}$) or infected with vector (Vector). Results shown are representative of ten experiments, performed with two C-cell lines derived from different mice.

$Rb1^{+/-}Nras^{+/-}$ mice had lost the remaining wild-type *Nras* allele (**Fig. 2k**; data not shown), 7 of which occurred in mice displaying distant metastases. Two of the fourteen mice harboring tumors where loss of *Nras* was not apparent displayed visible metastases. And in these associated metastases, loss of the remaining wild-type *Nras* allele was observed (**Fig. 2l**). In all tumors, regardless of *Nras* genotype or malignant status, loss of *Rb1* was invariant (data not shown). Further, in metastatic medullary carcinomas no evidence was observed for activating mutations in *Hras* or *Kras* (data not shown), indicating that such genetic events do not participate in the genesis of these tumors. These observations indicate that the development of large macroscopic C-cell tumors and associated metastases in $Rb1^{+/-}Nras^{+/-}$ mice is frequently associated with loss of the remaining wild-type *Nras* allele, suggesting that this genetic event is rate limiting for the acquisition of metastatic behavior by these tumors.

To determine the contribution of *Nras* nullizygosity to the metastatic potential of *Rb1*-deficient C cells, we injected single-cell suspensions derived directly from tumors arising in $Rb1^{+/-}Nras^{-/-}$ and $Rb1^{+/-}$ mice into the tail veins of nude mice. We have not successfully derived C-cell lines from tumors occurring in $Rb1^{+/-}Nras^{+/+}$ mice. As anticipated, in two such experiments using independent cell preparations only the *Nras*-deficient C cells developed metastases to the liver and lung (data not shown). In addition, C cells derived from a tumor that occurred in an $Rb1^{+/-}Nras^{-/-}$ mouse with no signs of metastasis metastasized upon tail vein injection (data not shown). To examine the influence of the tissue microenvironment on the possible selective pressure to lose the remaining *Nras* allele, we characterized C-cell lines derived from tumors occurring in $Rb1^{+/-}Nras^{-/-}$ and $Rb1^{+/-}Nras^{+/-}$ mice (**Fig. 3a**), neither of which showed evidence of loss of the remaining *Nras* allele. Subcutaneous injection of these lines gave rise to tumors regardless of *Nras* status and, notably, subcutaneous tumors derived from $Rb1^{-/-}Nras^{+/-}$ C cells continued to express N-Ras (**Fig. 3b**). By contrast, upon intravenous injection of the same lines $Rb1^{-/-}Nras^{-/-}$ C cells metastasized more efficiently compared to $Rb1^{-/-}Nras^{+/-}$ C cells (**Fig. 3c**). And in this setting, examination of C cells derived from the resultant liver metastases revealed that N-Ras protein expression and, correspondingly, the remaining *Nras* allele were lost (**Fig. 3d**). We then attempted the opposite experiment and observed that expression of N-Ras by lentiviral infection in $Rb1^{-/-}Nras^{-/-}$ C cells suppressed their ability to metastasize (**Fig. 3e**). Collectively, these data suggest that the state of *Nras* nullizygosity in *Rb1*-deficient C cells is an important cell-autonomous determinant in the ability of these cells to metastasize.

To begin to explore the means by which loss of *Nras* confers upon *Rb1*-deficient C cells the ability to metastasize, we considered various signaling events known to be affected by Ras, first comparing $Rb1^{-/-}Nras^{-/-}$ to $Rb1^{-/-}Nras^{+/-}$ C cells. These analyses revealed that RhoA activity was significantly higher in *Nras*-deficient C cells compared to those heterozygous for *Nras* (**Fig. 4a**). The effect was due to *Nras* nullizygosity and not events secondary to *Nras* loss, as restoration of N-Ras expression (**Fig. 4a**) reduced the activity of RhoA in $Rb1^{-/-}Nras^{-/-}$ C cells (**Fig. 4b**). Moreover, this was a specific property of wild-type N-Ras, as introduction of oncogenic N-Ras, N-Ras^{V12}, further elevated RhoA activity and dominant-negative N-Ras, N-Ras^{N17} and wild-type K-Ras had no effect (**Fig. 4b**). The activity of Rac and Cdc42 were not altered by the expression of N-Ras in $Rb1^{-/-}Nras^{-/-}$ C cells (**Fig. 4b**).

Given that Rho GTPases have been implicated in cell invasion[17], we determined whether *Rb1 Nras* mutant C cells possess the ability to invade into Matrigel in a Rho-dependent manner. $Rb1^{-/-}Nras^{-/-}$ C cells were found to be capable of invading Matrigel and expression of wild-type, but not oncogenic, N-Ras (N-Ras^{V12}) in these cells blocked this behavior (**Fig. 4c**). Likewise, expression of a dominant-negative RhoA mutant, $RhoA^{N19}$ (**Fig. 4b**), or treatment with C3 toxin (TAT-C3, ref. 17), which inactivates Rho, almost completely inhibited the invasion of *Rb1 Nras* mutant C cells (**Fig. 4c**). Treatment of cells

with Y-27632, an inhibitor of Rho kinases ROCKI and ROCKII, downstream effectors of RhoA, also significantly attenuated the migratory behavior of *Rb1 Nras* mutant C cells, albeit not to the same degree as inhibition of RhoA (**Fig. 4c**). Extending these findings to an *in vivo* setting, we observed that inhibition of RhoA activity in $Rb1^{-/-}Nras^{-/-}$ C cells suppressed their ability to metastasize after intravenous injection into mice to a degree comparable to that found with introduction of wild-type N-Ras (**Figs. 4d** and **3e**). In aggregate, these data suggest that aberrantly elevated RhoA activity after loss of *Nras* in *Rb1*-deficient C cells contributes to the metastatic behavior of *Rb1 Nras* mutant C cells.

Despite the fact that *Nras* nullizygous mice are phenotypically normal and not prone to the development of tumors, our findings indicate that this proto-oncogene can have a profound impact on tumor progression. Further, our data indicate that *Nras* loss can inhibit pituitary adenocarcinomas, which are endocrine tumors, while promoting the malignant progression of C-cell tumors, which are of neuroendocrine origin, suggesting that the contribution of *Nras* to tumorigenesis is cell type–dependent. In the context of *Rb1* loss, this appears to be an emerging theme: for example, the cooperative effects of *Rb1* and *Trp53* loss are observed in the development of murine small-cell lung carcinoma[18], but not retinoblastoma[19]. In both the pituitary and thyroid the effect of the genetic interaction between *Rb1* and *Nras* is to influence the differentiation status of the tumor. In the case of our model of medullary thyroid carcinoma, it is intriguing to note that introduction of oncogenic Ras into cell lines derived from tumors of neuroendocrine origin, such as medullary thyroid carcinomas, small-cell lung carcinomas and pheochromocytomas (for example, PC12), promotes their differentiation[20–23], and that such tumors do not harbor activating mutations in Ras[24,25]. We would suggest that loss of *Nras* in C cells, in the context of *Rb1* deficiency, is associated with a less differentiated state and that this allows the acquisition of migratory and invasive behavior that C cells normally possess during embryogenesis, thereby contributing to their metastatic potential.

METHODS

Mice and genotyping. $Rb1^{+/-}$ and $Nras^{+/-}$ mice[5] were crossed to generate $Rb1^{+/-}Nras^{+/-}$ animals that were then crossed to yield mice used in this study. Genotyping by PCR was performed as described[6,26]. Nude mice (BALB/c *nu/nu*) were from Taconic or SLC. Establishment and observation of the *Rb1 Nras* cohort was performed at the Dana-Farber Cancer Institute Animal Resource Facility in accordance with the guidelines of the National Institutes of Health. Assays using nude mice were performed either at the Dana-Farber Cancer Institute, or at Kyoto University under the guidelines of Kyoto University.

Histology and immunohistochemistry. Isolated tumors were fixed in 4% paraformaldehyde in PBS and embedded in paraffin. Sections (6 μm) were stained with hematoxylin and eosin (H&E). Immunostaining was with polyclonal antibodies to ACTH (N1531; Dako), Calcitonin (N1552; Dako) or CEA (N1503; Dako) or monoclonal antibody to PCNA (PC10; Sigma). Counterstaining was with methyl green and DAPI staining with Vectashield (0.2 μg/ml; H-1200; Vector). For ACTH and CEA staining, the intensities of the signals in four fields were measured (NIH Image (1.61)) and relative values determined after setting value in $Rb1^{+/-}Nras^{+/+}$ mice to 1. For PCNA staining, the percentage of positive nuclei in four fields was determined. Nuclear to cytoplasmic ratio and DAPI levels were quantified (NIH Image (1.61)) in 50 randomly chosen cells. Double indirect immunofluorescence for PCNA and ACTH was with the above primary antibodies and rhodamine-conjugated and FITC-conjugated secondary antibodies, respectively (Jackson Immunoresearch Laboratories).

C-cell culture and infection. To establish C-cell lines, tumors were surgically separated from thyroid glands, minced with a surgical blade and suspended in DMEM containing 0.5% trypsin and 0.53 mM EDTA at 4 °C. After 12 h incubation cells were resuspended in DMEM supplemented with 10% FBS (JRH Biosciences), 10% horse serum (Invitrogen), 10 μg/ml insulin and 10 μg/ml transferrin. cDNAs encoding N-Ras, $N\text{-}Ras^{V12}$, $N\text{-}Ras^{N17}$, K-Ras and $RhoA^{N19}$ (Lumio tagged (Invitrogen) at their N terminus to monitor expression *in vivo*) were subcloned into pLenti6/V5 and virus generated using ViraPower LentiViral Expression System (Invitrogen). Expression of the encoded proteins was determined using monoclonal antibodies to N-Ras (OP25; Oncogene), K-Ras (234-4.2; Sigma) or RhoA (26C4; Santa Cruz Biotechnology).

Southern analysis. For determination of the *Nras* status, tumor and normal (tail) DNA was digested with *Eco*RI and hybridized with a probe derived from the first intron of the *Nras* gene[8].

***In vitro* invasion assay.** Invasion chambers (Chemotaxicell from Karabo) with 8-μm porous polycarbonate membranes were coated with Matrigel (354234; BD Biosciences). Ten-thousand infected or treated cells were plated in the upper chamber in Opti-MEM (Invitrogen) containing 0.8% bovine serum albumin, 1% FBS and 1% horse serum. The lower chamber was filled with Opti-MEM containing 5% FBS and 5% horse serum. After 72 h incubation we collected cells invading into the bottom chamber, stained them with antibody against calcitonin and counted the number of invading C cells in ten fields under 40× magnification. TAT-C3 (a gift from E. Sahai and C. Marshall) was prepared as described[17]. Y-27632 was from Calbiochem.

RhoA, Rac and Cdc42 activity assays. Pull-down assays to measure RhoA, Rac and Cdc42 activity were performed as described[27,28].

Note: Supplementary information is available on the Nature Genetics website.

ACKNOWLEDGMENTS

We thank T. Jacks, R. Kucherlapati and A. Silva for providing mice; F. Giancotti, H. Kitayama, C. Marshall, S. Narumiya, X.-D. Ren, E. Sahai, M. Schwartz and M. Symons for useful reagents; A. Tischler, P. Fotiadou, D.M. Livingston, A. Shamma, T. Miki and C. Das for critical reading of the manuscript; K.-Y. Lee, J. Suh, C. McMahon, J. Lamb, W. Sellers, R. Takahashi and H. Rajabi for advice and encouragement. This work was supported by funding from the National Cancer Institute–Japanese Foundation for Cancer Research Scientist Exchange Program, Massachusetts Prostate Cancer Research Program, Japanese Ministry of Education, Culture, Sports, Science and Technology, The 21st Century Center of Excellence Program, Yamanouchi Foundation for Research on Metabolic Disorders and Public Trust Haraguchi Memorial Cancer Research Fund (C.T.) and the National Cancer Institute (M.L. and M.E.E.).

COMPETING INTERESTS STATEMENT

The authors declare that they have no competing financial interests.

Published online at http://www.nature.com/naturegenetics/
Reprints and permissions information is available online at http://npg.nature.com/reprintsandpermissions/

1. Fearon, E.R. Human cancer syndromes: clues to the origin and nature of cancer. *Science* **278**, 1043–1050 (1997).
2. Vooijs, M. & Berns, A. Developmental defects and tumor predisposition in *Rb* mutant mice. *Oncogene* **18**, 5293–5303 (1999).
3. Zhang, Z. *et al.* Wildtype *Kras2* can inhibit lung carcinogenesis in mice. *Nat. Genet.* **29**, 25–33 (2001).
4. Lee, K.Y., Ladha, M.H., McMahon, C. & Ewen, M.E. The retinoblastoma protein is linked to the activation of Ras. *Mol. Cell. Biol.* **19**, 7724–7732 (1999).
5. Takahashi, C. *et al. Rb* and N-*ras* function together to control differentiation in the mouse. *Mol. Cell. Biol.* **23**, 5256–5268 (2003).
6. Jacks, T. *et al.* Effects of an *Rb* mutation in the mouse. *Nature* **359**, 295–300 (1992).
7. Williams, B.O. *et al.* Cooperative tumorigenic effects of germline mutations in *Rb* and *p53*. *Nat. Genet.* **7**, 480–484 (1994).
8. Umanoff, H., Edelmann, W., Pellicer, A. & Kucherlapati, R. The murine N-*ras* gene is not essential for growth and development. *Proc. Natl. Acad. Sci. USA* **92**, 1709–1713 (1995).
9. Hu, N. *et al.* Heterozygous *Rb*-1 delta 20/+ mice are predisposed to tumors of the pituitary gland with a nearly complete penetrance. *Oncogene* **9**, 1021–1027 (1994).
10. Harrison, D.J., Hooper, M.L., Armstrong, J.F. & Clarke, A.R. Effects of heterozygosity for the $Rb\text{-}1^{t19neo}$ allele in the mouse. *Oncogene* **20**, 1615–1620 (1995).
11. Capen, C.C. *et al.* in *International Classification of Rodent Tumors: The Mouse* (ed. Mohr, U.) 269–322 (Springer-Verlag, Germany, 2001).

12. White, A. & Gibson, S. ACTH precursors: biological significance and clinical relevance. *Clin. Endocrinol.* **48**, 251–255 (1998).
13. Mills, S.E. Neuroectodermal neoplasms of the head and neck with emphasis on neuroendocrine carcinomas. *Mod. Pathol.* **15**, 264–278 (2002).
14. Beskid, M. C cell adenoma of the human thyroid gland. *Oncology* **36**, 19–22 (1979).
15. Kodama, T. *et al.* C cell adenoma of the thyroid: a rare but distinct clinical entity. *Surgery* **104**, 997–1003 (1988).
16. Takahashi, C., Contreras, B., Bronson, R.T., Loda, M. & Ewen, M.E. Genetic interaction between *Rb* and K-*ras* in the control of differentiation and tumor suppression. *Mol. Cell. Biol.* **24**, 10406–10415 (2004).
17. Sahai, E. & Marshall, C.J. Differing modes of tumour cell invasion have distinct requirements for Rho/ROCK signalling and extracellular proteolysis. *Nat. Cell Biol.* **5**, 711–719 (2003).
18. Meuwissen, R. *et al.* Induction of small cell lung cancer by somatic inactivation of both *Trp53* and *Rb1* in a conditional mouse model. *Cancer Cell* **4**, 181–189 (2003).
19. MacPherson, D. *et al.* Cell type-specific effects of *Rb* deletion in the murine retina. *Genes Dev.* **18**, 1681–1694 (2004).
20. Nakagawa, T. *et al.* Introduction of v-Ha-ras oncogene induces differentiation of cultured human medullary thyroid carcinoma cells. *Proc. Natl. Acad. Sci. USA* **84**, 5923–5927 (1987).
21. Bar-Sagi, D. & Feramisco, J.R. Microinjection of the ras oncogene protein into PC12 cells induces morphological differentiation. *Cell* **42**, 841–848 (1985).
22. Mabry, M. *et al.* Insertion of the v-Ha-ras oncogene induces differentiation of calcitonin-producing human small cell lung cancer. *J. Clin. Invest.* **84**, 194–199 (1989).
23. Noda, M. *et al.* Sarcoma viruses carrying ras oncogenes induce differentiation-associated properties in a neuronal cell line. *Nature* **318**, 73–75 (1985).
24. Moley, J.F. *et al.* Low frequency of ras gene mutations in neuroblastomas, pheochromocytomas, and medullary thyroid cancers. *Cancer Res.* **51**, 1596–1599 (1991).
25. Mitsudomi, T. *et al.* Mutations of ras genes distinguishes a subset of non-small-cell lung cancer cell lines from small-cell lung cancer lines. *Oncogene* **6**, 1352–1362 (1991).
26. Johnson, L. *et al.* K-*ras* is an essential gene in the mouse with partial functional overlap with N-*ras*. *Genes Dev.* **11**, 2468–2481 (1997).
27. Ren, X.-D., Kiosses, W.B. & Schwartz, M.A. Regulation of the small GTP-binding protein Rho by cell adhesion and the cytoskeleton. *EMBO J.* **18**, 578–585 (1999).
28. Mettouchi, A. *et al.* Integrin-specific activation of Rac controls progression through the G1 phase of the cell cycle. *Mol. Cell* **8**, 115–127 (2001).